Determination of the optical constants of MgF_2 and ZnS from spectrophotometric measurements and the classical oscillator method

Jesus M. Siqueiros, Roberto Machorro, and Luis E. Regalado

The values of the optical constants of magnesium fluoride (MgF_2) and zinc sulfide (ZnS) thin films are obtained using a classical oscillator model and the experimental values of their spectral transmittance. Auger electron spectroscopy was performed on the samples to determine the chemical composition of the films. These materials are important in the design of filters, mirrors, and antireflection coatings for optical instrumentation. Unfortunately their properties strongly depend on evaporation conditions. The procedure described here allows direct measurement of the dispersive refractive index of the film after deposition.

I. Introduction

There are many ways reported in the literature[1-6] to determine the optical properties of thin films of different materials from spectrophotometric measurements, that is, spectral transmittance and reflectance. The classical oscillator model used in this work[7] may be particularly suited for dielectric thin films and, within a restricted frequency interval, for semiconductors as well. The most relevant features of this method are its ability to produce good values of optical constants from experimental data and the possibility of attributing a real physical meaning to the parameters of the oscillators representing the optical properties of the material.

A transparent dielectric (MgF_2) and a semiconductor (ZnS) are suitable materials for the use of this technique since they fill very well the above-mentioned requirements for its application and because there are sufficient available data in the literature with which to compare the results.

II. Theory

Representing the complex dielectric function as a sum of classical oscillators, it is possible to reproduce the transmittance and reflectance curves of a solid in the spectral region corresponding to the lattice vibration.[8] We can write

$$\varepsilon = \varepsilon_1 + \varepsilon_2 = \varepsilon_\infty + \sum S_i/[(1 - \omega^2/\omega_i^2) - j\gamma_i\omega/\omega_i], \qquad (1)$$

where S_i, ω_i, and γ_i represent, respectively, the strength, resonance frequency, and linewidth of the actuating oscillators. The high frequency dielectric constant ε_∞ represents the contribution to ε from high frequency transitions. The knowledge of one or more of these sets of four parameters will permit us to calculate theoretical values of reflectance and transmittance and to compare them to experimental data to find the best-fitted values of ε as a function of ω, from Eq. (1).

III. Sample Preparation and Characterization

MgF_2 and ZnS films were thermally evaporated on BK7 substrates at room temperature in a $5\text{-} \times 10^{-6}$-Torr vacuum. The pressure may increase to the 10^{-5} range during evaporation. The deposition rates were 4 and 9 nm/s, respectively. The film thickness was controlled during deposition using a reflectance–transmittance (R/T) optical monitor. Due to geometrical limitations, only 3-cm diam substrates had been used, where a thickness uniformity better than 98% can be achieved. The samples studied have optical thicknesses that are multiple integers of the monitoring wavelength, that is, the shutter is closed to stop the evaporation at a turning point of the R/T signal vs optical thickness.

Even though the optical monitor inside the evaporation chamber gives us an estimate of the film thickness, it was measured again by two alternative techniques: (i) using a multiple beam Tolansky interferometer[9]

Jesus Siqueiros is with IFUNAM, Labortorio de Ensenada, A.P. 2661, Ensenada, BC. Mexico; R. Machorro is with CICESE, A.P. 2732, Ensenada, BC. Mexico; and L. E. Regalado is with CIF-US Universidad de Sonora, A.P. A-88, Hermosillo, Son., Mexico.

Received 8 June 1987.
0003-6935/88/122549-05$02.00/0.

© 1988 Optical Society of America.

Table I. Film Thickness Measurement Comparison

Technique	Measured geometrical thickness (nm)	
	MgF_2	ZnS
Manifacier[3]	227	265
Tolansky[7]	225	251
Optical monitor	222	262
Oscillator model	230	236

and (ii) using the maxima and minima of spectrophotometric spectra, following Manifacier's technique.[3,10] We found good agreement between the results given by these techniques, as shown in Table I.

Spectral transmittance on both materials was measured in a Perkin-Elmer model 330 spectrophotometer, which has a double beam, one for the sample and one for reference. In our case the reference is air, and the computer program makes the compensation for the second surface and thickness of the substrate. The relative precision of wavelength is better than 1% at 200-nm/min scan speed and the photometric accuracy is 0.3% in transmittance.

Samples were also analyzed by Auger electron spectroscopy to obtain their physicochemical properties, stoichiometry, and the presence of possible contaminants. Auger spectra are shown in Figs. 1 and 2.

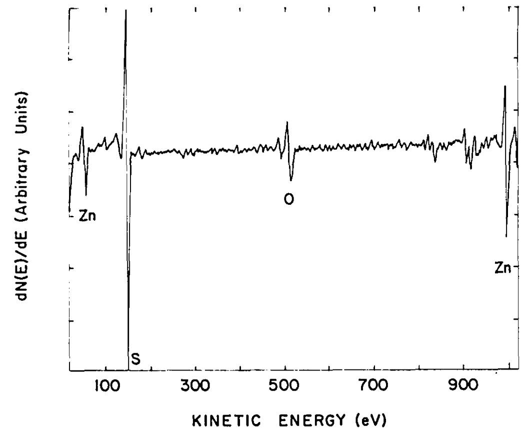

Fig. 1. Auger spectrum for ZnS showing very clean samples.

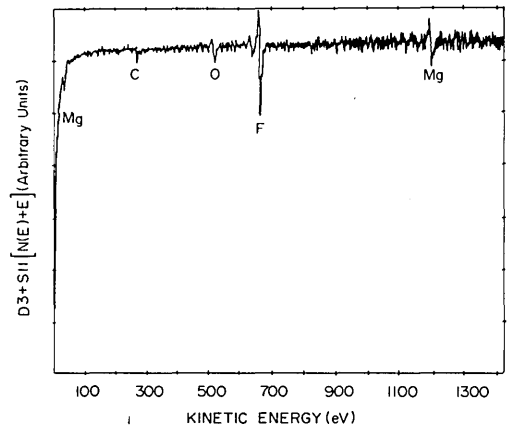

Fig. 2. Auger spectrum for MgF_2 near the surface. The third derivative was used to detect electrically isolated films.

IV. The R/T Calculations

Reflectance (R) and transmittance (T) of a thin film can be calculated by repeated use of the boundary conditions for the electromagnetic fields plus the interference effects of the fields traveling in both directions across the film and reflected in the interfaces of the different media.[11]

The R and T calculations may be done in several different ways, for example, using characteristic or transfer matrix theory, developed by Abeles[12] or using recurrent formulas based on Airy's expression. In this work we follow a simple form of the computational procedure developed by Dupoisot and Morizet[13] adapted to a single film. This calculation is also modified to include the second surface effects. Waves reflected successively on the first and second surfaces add up incoherently for thick glass substrates compared to the coherence length of the light source being used.[11]

V. Search Process for the Best Set of Parameters

There are many possible solutions to the problem of finding the best set of parameters based on experimental data; some are reported in Refs. 1–6. We propose the use of the least-squares method for an arbitrary function[14]; in our case this function is the recurrence formula:

$$T = (n_s/n_o)(\tau\tau^*), \tag{2}$$

where τ^* is the conjugate of $\tau_{j-1} = t_{j-1}\exp(2\psi_j)\tau_j/\exp(2\psi_j) + r_{j-1}\rho_j$. The aim is to find the optimum set of parameters, so that the differences between the experimental and calculated data (transmittances) are minimum. We can define the objective function M by

$$M = \sum_{k=1}^{N} (T_c - T_e)^2_k, \tag{3}$$

where T_c is the transmittance obtained from the recurrence formula, and T_e is the corresponding experimental value. The numerical value of the objective function M gives us a measure of the goodness of the fit.

The search is done using a $3n + 1$ dimension grid, where n is the number of oscillators, and the extra dimension stands for the ε_∞. Assuming that the variation of M with each parameter is independent of the optimization degree with respect to the others, the best set of parameters may be determined by the minimization of M with respect to each parameter separately. The main disadvantage of this technique is that the parameters may not be independent, which means that the problem may not have a unique solution.

In the optimization process each parameter y_i is incremented by a prescribed amount Δy_i, whose sign is chosen so that the corresponding M, denoted by M_i, decreases. The process continues until $M_i < M_{i+1}$. Assuming the variation of M, near the minimum, is a

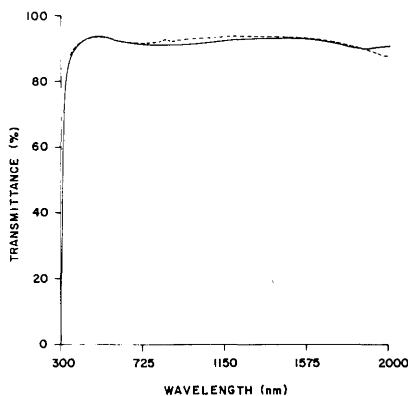

Fig. 3. Optical spectrum of MgF_2. Low contrast fringes are caused by the similarity of refractive index of both the film and the glass substrate.

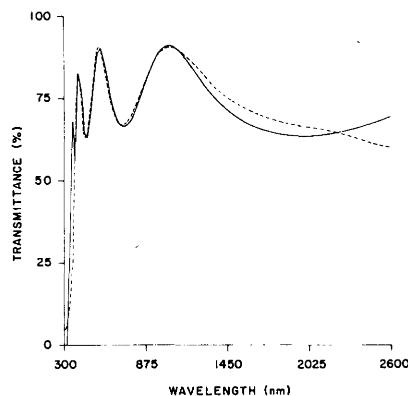

Fig. 4. The ZnS optical spectrum presenting good contrast between maxima and minima in transmittance.

parabolic function of the current parameter y_i under optimization, the last three points (M_i,y_i) can be used to get the minimum of the parabola. This procedure is repeated for each parameter, and the iteration goes on until the changes in M_i are smaller than a given uncertainty.

The order in which the parameters are optimized is important, and sometimes it is convenient to fix some of them. Spitzer and Kleinmann[7] suggested a way of selecting the initial parameters, based on inspection of the experimental data. In our program we introduce the possibility to weigh and fix some parameters as a measure of their influence on M.

VI. Results and Discussion

From the Auger spectra, Figs. 1 and 2, we observe that we have fairly clean films for both MgF_2 and ZnS, and according to the Auger sensitivity manual,[15] our materials are closely stoichiometric.

Before working on sample films, we obtained the complex dielectric function for the BK7 substrate using the same oscillator modeling. The resulting values were taken into account in the calculation of the dispersion curve of the films. The oscillator values for the substrate are:

high frequency dielectric constant $\varepsilon_\infty = 2.13$,

oscillator frequencies $\omega_1 = 4.10$ eV $\omega_2 = 0.44$ eV $\omega_3 = 1.2$ eV,

oscillator strength $S_1 = 0.23$ $S_2 = 0.7$ $S_3 = 4.9$,

oscillator linewidth $\gamma_1 = 0.0005$ eV $\gamma_2 = 0.5$ eV $\gamma_3 = 11.0$.

The optical spectrum for MgF_2, Fig. 3, shows almost no structure, except for the ultraviolet region where a strong tendency toward a minimum is evident. The interference oscillations characteristic of film thickness are very weak but, nevertheless, they can be observed in the spectrum whose maxima and minima give a film thickness of 227 nm following Manifacier's technique.[3] This value is in agreement with the thickness measured in a Tolansky interference microscope, the difference being of the order of the surface irregularities. From the methods used, only the multiple beam technique provides a direct measurement of the geometrical thickness. The optical thickness is divided by the refractive index taken from Macleod,[11] at the monitoring wavelength, to make the comparison. This value is used as a starting point in the algorithm and will be optimized as well. The resulting thicknesses are presented in Table I.

Once the thickness of the film is estimated, we proceed with the search for a set of parameters that fits the experimental data. For MgF_2 we have obtained two oscillators:

high frequency dielectric constant $\varepsilon_\infty = 1.65$,

oscillator frequencies $\omega_1 = 6.5$ eV $\omega_2 = 0.4$ eV,

oscillator strength $S_1 = 0.1$ $S_2 = 0.5$,

oscillator linewidth $\gamma_1 = 0.05$ eV $\gamma_2 = 8.0$ eV.

The high energy oscillator (6.5 eV) is responsible for the UV transmission minimum, while the low energy oscillator (0.4 eV) produces a bending of the transmission curve toward the infrared region.

In the case of ZnS, for the calculated thickness of 236 nm we also have two oscillators:

high frequency dielectric constant $\varepsilon_\infty = 4.4$,

oscillator frequencies $\omega_1 = 3.8$ eV $\omega_2 = 0.27$ eV,

oscillator strength $S_1 = 0.8$ $S_2 = 0.9$,

oscillator linewidth $\gamma_1 = 0.005$ eV $\gamma_2 = 1.2$ eV.

The strong absorption shown in the high frequency region, Fig. 4, may be related to the energy band gap, reported to be 3.6 eV.[16] For our sample, the oscillator had a band gap energy of 3.8 eV. The low energy (0.27-eV) oscillator bends the transmittance curve as seen in the infrared part of the spectrum.

Once the dielectric function has been computed, the complex refractive index may be easily determined, using relation $\varepsilon = n^2$, where n is, in general, a complex number. Our results for the wavelength dispersion are shown in Fig. 5 for MgF_2 and in Fig. 6 for ZnS.

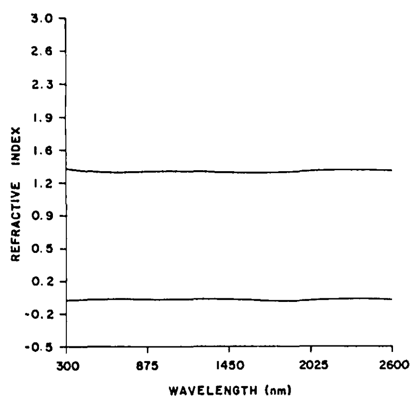

Fig. 5. Real and imaginary parts of the refractive index for MgF_2 calculated from the best-fitted parameters from two contributing oscillators.

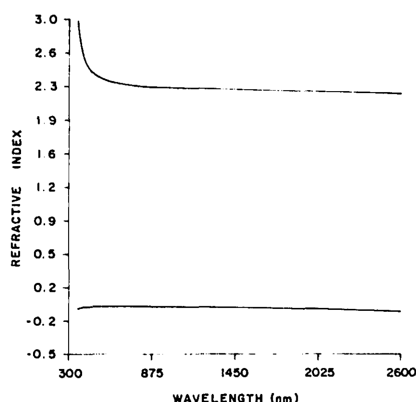

Fig. 6. Complex refractive index for ZnS. The dispersion is higher for the UV region. Two oscillators contribute to this calculation.

It may be useful to compare the resulting complex refractive index with previous published data, as shown in Tables II and III. As can be seen, our values for the real part of the index for the MgF_2 are slightly lower than the cited values. This may be attributed to our deposition technique, since we evaporated on room temperature substrates rendering less closely packed films. Note that some of the cited figures are from bulk crystalline material.

VII. Conclusions

We have used an algorithm to obtain the dielectric constant of a thin film, as a function of wavelength, in terms of a sum of classical oscillators. This value was modified to fit experimental and calculated transmittances, yielding a dispersion curve. The method was successfully applied to a transparent dielectric, MgF_2, and a semiconductor, ZnS. The dispersion curves were also used to provide information about the band gap of the film material; this is particularly useful for dielectric and semiconductor materials.

The calculated dispersion for both materials was in good agreement with previous results.[1,17-19] This technique has been successfully tried in other semiconductors, such as ITO, amorphous and crystalline selenium, and cerium fluoride; the results will be reported separately. This method may be improved if reflectance measurements are also taken into account.

Table II. MgF_2 Refractive Index Dispersion

Wavelength (nm)	Model n	Model k	n	Reference No.
210	1.52	0.048		
270	1.40	0.0057		
310	1.38	0.0038		
370	1.37	0.0031		
400	1.37	0.0030		
404.6	1.37	0.0030	*1.384/1.395	18
501.5	1.37	0.0033	*1.379/1.392	18
511	1.36	0.0034		
550	1.36	0.0036	1.38	11
600	1.36	0.0040		
623.5	1.36	0.0040	*1.377/1.388	18
700	1.36	0.0046		
706.5	1.36	0.0047	*1.376/1.387	18
800	1.36	0.0053		
900	1.36	0.0061		
1000	1.36	0.0070		
1100	1.36	0.0077		
1200	1.36	0.0085		
1300	1.36	0.0093		
1400	1.36	0.0100		
1500	1.36	0.0110		
1600	1.36	0.0120		
1700	1.36	0.0120		
1800	1.36	0.0130		
1900	1.36	0.0140		
2000	1.36	0.0150	1.35	11

* Bulk crystalline form, ordinary and extraordinary indices, n_o and n_e.

Table III. ZnS Refractive Index Dispersion

Wavelength (nm)	Model n	Model k	n	Reference No.
400	2.61	0.0058	*2.564/2.56	18
500	2.41	0.0020	*2.425/2.421	11
550	2.37	0.0016	2.35	11
600	2.35	0.0014	*2.368/2.363	18
633	2.34	0.0014	2.33	19
700	2.32	0.0015	*2.337/2.332	18
800	2.31	0.0018	*2.328/2.324	18
900	2.30	0.0022	*2.315/2.310	18
1000	2.29	0.0028	*2.303/2.301	18
1100	2.29	0.0036		
1200	2.28	0.0046	*2.294/2.290	18
1300	2.28	0.0058		
1400	2.27	0.0072	*2.288/2.285	18
1500	2.27	0.0089		
1600	2.27	0.0107		
1700	2.26	0.0130		
1800	2.26	0.0154		
1900	2.26	0.0182		
2000	2.25	0.0213	2.2	11

* Bulk crystalline form, ordinary and extraordinary indices, n_o and n_e.

We would like to thank L. Cota (IFUNAM) for the Auger spectra analysis and useful discussions and D. Salazar (CICESE) for the sample preparation. One of the authors, LER, gratefully acknowledges the economical support of Direccion General de Investigacion

Cientifica y Superacion Academica (DGICSA-SEP). RM thanks CICESE since this work was done during his sabbatical leave at INAOE Puebla.

References

1. E. Pelletier, P. Roche, and B. Vidal, "Determination automatique des constants optiques et de l'épaisseur de couches minces: application aux couches diélectriques," Nouv. Rev. Opt. **7**, 353 (1976).
2. A. Hjortsberg, "Determination of Optical Constants of Absorbing Materials Using Transmission and Reflection of Thin Films on Partially Metallized Substrates: Analysis of the New (T,R_m) Technique," Appl. Opt. **20**, 1254 (1981).
3. J. C. Manifacier, J. Gasiot, and J. P. Fillard, "A Simple Method for the Determination of the Optical Constants n,k and the Thickness of a Weakly Absorbing Thin Film," J. Phys. E **9**, 1002 (1976).
4. R. J. King and S. P. Talim, "A Comparison of the Thin Film Measurement by Wave Guide, Ellipsometry and Reflectometry," Opt. Acta **28**, 1107 (1981).
5. J. M. Bennett and M. J. Booty, "Computational Method for Determining n and k for a Thin Film from the Measured Reflectance, Transmittance, and Film Thickness," Appl. Opt. **5**, 41 (1966).
6. D. P. Arndt *et al.*, "Multiple Determination of the Optical Constants of Thin-Film Coating Materials," Appl. Opt. **23**, 3571 (1984).
7. W. G. Spitzer and D. A. Kleinmann, "Infrared Lattice Bands of Quartz," Phys. Rev. **121**, 1324 (1961).
8. H. W. Verleur, "Determination of Optical Constant from Reflectance or Transmittance Measurements on Bulk Crystal or Thin Films," J. Opt. Soc. Am. **58**, 1356 (1968).
9. S. Tolansky, *Multiple Beam Interferometry of Surfaces and Films* (Clarendon, Oxford, 1948).
10. A. M. Goodman, "Optical Interference Method for the Approximate Determination of Refractive Index and Thickness of a Transparent Layer," Appl. Opt. **17**, 2779 (1978).
11. H. A. Macleod, *Thin-Film Optical Filters* (Adam Hilger, Bristol, 1986).
12. F. Abeles, "Transmission of Light by a System of Alternate Layers," C. R. Acad. Sci. **226**, 1808 (1948).
13. H. Dupoisot and J. Morizet, "Thin Film Coatings: Algorithms for the Determination of Reflectance and Transmittance, and Their Derivatives," Appl. Opt. **18**, 2701 (1979).
14. P. R. Bevington, *Data Reduction and Error Analysis for the Physical Sciences* (McGraw-Hill, New York, 1969).
15. L. E. Davis *et al.*, *Handbook of Auger Electron Spectroscopy* (Electronic Industries, Inc., Eden Prairie, MN, 1978).
16. C. Kittel, *Introduction to Solid State Physics* (Wiley, New York, 1976), p. 210.
17. S. Ogura, N. Sugawara, and R. Higara, "Refractive Index and Packing Density for MgF_2: Correlation of Temperature Dependence with Water Sorption," Thin Solid Films **30**, 3 (1975).
18. B. H. Billings, "Optics," in *American Institute of Physics Handbook*, D. E. Gray, Ed. (McGraw-Hill, New York, 1972), Chap. 6.
19. R. P. Netterfield, "Refractive Indices of Zinc Sulfide and Cryolite in Multilayer Stacks," Appl. Opt. **15**, 1969 (1976).

NASA *continued from page 2545*

Compact sun-position sensor

A light sensor combines a wide field of view with high resolution so that it can be used for both finding and tracking a moving light source like the sun. The sensor was developed as a smaller, lighter, and simpler replacement for an instrument that employed two sensors—one with coarse resolution and a wide field for finding the sun and one with fine resolution and a narrow field for following the moving sun after it has been found. Previously, the integration of the two types of sensor introduced mechanical and electronic complexity.

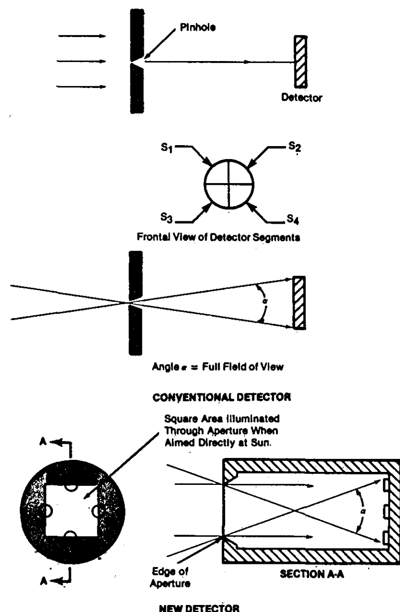

Fig. 5. Conventional sensor (above) can have a wide field of view or high angular resolution but not both. The new sensor (below) has both a wide field of view and high angular resolution when its axis is within a few degrees of the line to the sun.

A conventional sun-position sensor (see top of Fig. 5) includes a single photodetector divided into four quadrants, on which a spot of light is projected from a pinhole aperture. To increase the field of view, the diameter of the detector can be increased, or the distance between the aperture and detector can be decreased. However, the diameter should be small to keep noise and response time short. Moreover, decreasing the aperture distance makes the detector less sensitive to changes in spot position. Thus, a wide field of view is incompatible with high resolution. The new sensor contains four photodetectors spaced 90° apart on a circle opposite the square aperture of a small cylindrical chamber (see bottom of Fig. 5). The aperture casts equal shade on the detectors when the cylinder axis points directly at the center of the sun. Upward or downward movement of the sun places one of the vertical-motion detectors in more shade and the other in less shade. The difference in the outputs of the two vertical-motion detectors S_1 and S_3 is therefore an elevation-error signal. Similarly, sideways motion of the sun changes the shade on each of the horizontal detectors relative to the other so that S_2 and S_4 generate an azimuth-error signal. The detectors can be photovoltaic cells or photoresistors.

This work was done by Yutaka Matsumoto and Cesar Mina of Ames Research Center. Inquiries concerning rights for the commercial use of this patent should be addressed to the Patent Counsel, Ames Research Center, D. G. Brekke, Mail Code 200-11, Moffett Field, CA 94035. Refer to ARC-11696.

Optical rotary joint for data transfer

A scheme for transferring digital data across a rotary joint would use light instead of electrical signals. The optical joint would offer greater bandwidth than that of conventional electrical slip rings and would probably operate at a considerably lower error rate. Accord-

continued on page 2579